20

Fluorescent Energy Transfer Readout of an Aptazyme-Based Biosensor

David Rueda and Nils G. Walter

Summary

Biosensors are devices that amplify signals generated from the specific interaction between a receptor and an analyte of interest. RNA structural motifs called aptamers have recently been discovered as receptor components for biosensors owing to the ease with which they can be evolved in vitro to bind a variety of ligands with high specificity and affinity. By coupling an aptamer as allosteric control element to a catalytic RNA such as the hammerhead ribozyme, ligand binding is transduced into a catalytic event. We have made use of fluorescence resonance energy transfer (FRET) to further amplify ligand induced catalysis into an easily detectable fluorescence signal. This chapter reviews in detail the methods and protocols to prepare a theophylline specific aptazyme and to label its substrate with fluorophores. We also include detailed protocols to characterize by FRET the binding affinity of the target, theophylline, as well as the external substrate to the aptazyme. The chapter should therefore facilitate the implementation of RNA-based biosensor components for other analytes of interest.

Key Words: Allostery; aptamer; aptazyme; asthma; biosensor; bronchodilator; catalytic RNA; fluorescence resonance energy transfer; FRET; hammerhead ribozyme; theophylline.

1. Introduction

The ability to quantify the concentrations of drugs, second messengers, hormones, and proteins is of fundamental biomedical importance. Although DNA microarray chips are revolutionizing biology by expanding our analyses from single-gene to genome-wide gene expression, analogous methods for the simultaneous study of the metabolome and proteome are not yet available. In addition, rapid monitoring of cellular events such as second messenger synthesis and hormone secretion in single cells is key to understand cellular organization in higher organisms, yet is still not fully accomplished. Finally, early

From: *Methods in Molecular Biology, vol. 335:*
Fluorescent Energy Transfer Nucleic Acid Probes: Designs and Protocols
Edited by: V. V. Didenko © Humana Press Inc., Totowa, NJ

pathogen detection is of increasing urgency in clinical diagnosis and biodefense in the face of newly emerging infectious diseases. For these applications, new biosensor technologies are needed.

Biosensors are hybrid analytical devices that amplify signals generated from the specific interaction between a receptor and an analyte of interest, through a biophysical mechanism. Biosensors use tissues, whole cells, artificial membranes, or cell components like proteins or nucleic acids as receptors, coupled to a physicochemical signal transducer. The ideal biosensor is extremely sensitive, specific for the target of interest, adaptable to a wide range of target analytes, compact, rugged, and consumes very little energy or other resources.

Particularly notorious targets for biosensors are small organic compounds such as theophylline (**Fig. 1B**). Theophylline is a bronchodilating drug widely used in the treatment of asthma, bronchitis, and emphysema, with a narrow therapeutic range ***(1)***. Its serum levels must, therefore, be monitored carefully to avoid toxicity. Detection of theophylline is particularly challenging because of its resemblance to the ubiquitous caffeine, which carries only one additional methyl group on the N7 of the purine ring (**Fig. 1B**).

RNA is a unique biopolymer in that it can carry genetic information, encoded in its linear sequence, and can bind ligands or substrates specifically, even catalyze chemical reactions, based on its ability to fold into complex three-dimensional structures. The high thermodynamic stability of the secondary structure (Watson-Crick basepairing) of RNA provides for a stable scaffold to acquire diverse tertiary structures that can recognize ligands with extremely high specificity and sensitivity, in some cases even surpassing those of antibodies ***(2)***. As a consequence, RNA has recently been proposed as ligand-specific receptor component for biosensors ***(3–5)***, and even nature herself appears to resort to such RNA-based sensing ***(6)***.

RNA structural motifs called aptamers can be evolved in vitro to bind a desired ligand with high selectivity and tight binding affinity ***(2)***. The modularity of RNA structure allows one to incorporate aptamers into larger RNAs without loss of their binding properties. Breaker and co-workers have exploited this property to develop an allosteric RNA comprised of three elements: an aptamer as ligand receptor, a catalytic RNA called the hammerhead ribozyme as amplifier, and a communication module to couple their functions ***(4,7–12)***. Specifically, the aptamer and the communication module are incorporated into stem II of the hammerhead ribozyme in a way that catalytic activity is enhanced when the ligand binds. Such allosterically activated ribozymes are called aptazymes. **Figure 1A** shows the signal transduction mechanism for this aptazyme. In the absence of theophylline, the communication module is in a misaligned basepairing pattern, and the aptazyme-substrate complex is catalytically inactive. Upon addition of theophylline, the aptamer undergoes a con-

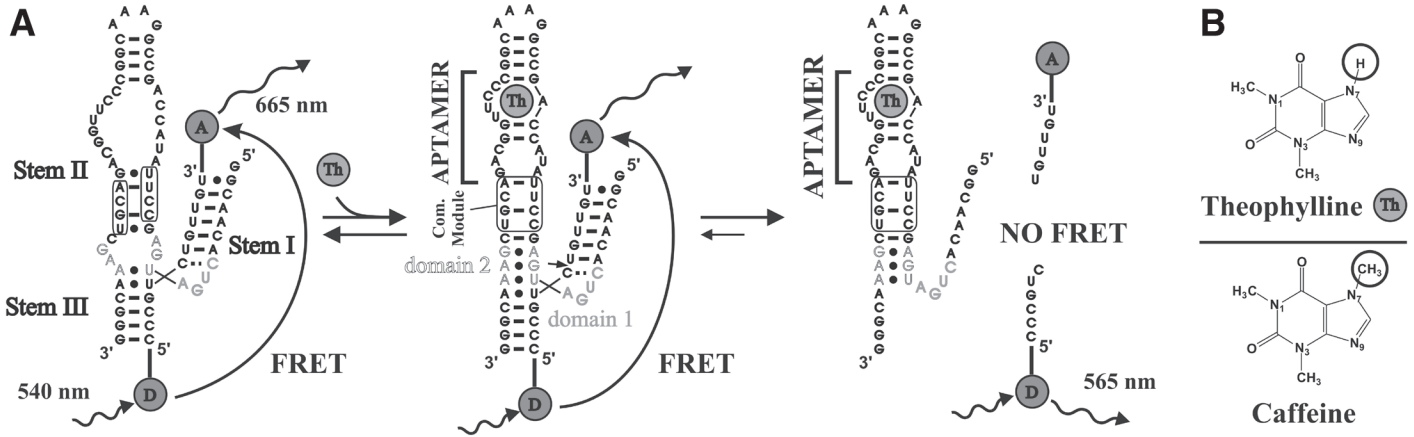

Fig. 1. Reaction pathway of the theophylline dependent aptazyme. **(A)** In the absence of theophylline (**Left**), the aptazyme–substrate complex is in a catalytically inactive conformation because the communication module (boxed) is misaligned. The characteristic high fluorescence resonance energy transfer (FRET) efficiency results in strong acceptor emission at 665 nm. Upon binding of theophylline (**Middle**), the catalytically active conformation of the ribozyme is formed by the realignment of the communication module (box). This event induces formation of domain 2, which is required for activity of the hammerhead ribozyme ***(14)***. Substrate cleavage occurs at the arrow, and the rapid dissociation of the 5' and 3' products follows (**Right**). The resulting separation of the fluorophores decreases FRET, and the donor emission at 565 nm increases at the expense of acceptor emission at 665 nm. **(B)** Chemical structures of theophylline and caffeine. The circles highlight their only difference: a methyl group on N7, which is distinguished by our aptazyme.

formational change ***(13)***, which aligns the communication module so that two adjacent G-A basepairs and a noncanonical A-U basepair in domain 2 of the hammerhead ribozyme can coaxially stack ***(14)***. Consequently, the catalytically active conformation is accessed, the substrate backbone is cleaved, and the reaction products are released.

Although classically ribozyme activity induced by allosteric binding has been detected by radioisotope labeling ***(4)***, the use of fluorophores provides an attractive alternative for the following reasons: (1) Fluorophores do not carry the inherent risks in handling and disposal of radiolabeled nucleotides. (2) Fluorescence can be easily monitored and quantified directly in solution, whereas radioisotope assays require discontinuous analysis. Therefore, fluorescence detection accelerates the analysis process. (3) Large numbers of samples can be measured in short periods of time because microplate fluorescence readers and further miniaturized microarrays enable automation of the detection process. (4) The fluorescence probe shelf life is virtually unlimited compared to radioisotopes, which decay over time. In general, we have found fluorescence spectroscopy to be a versatile probe for studying cleavage kinetics and conformational changes of catalytic RNAs ***(15–23)***.

With this in mind, we have developed a biosensor component for theophylline based on the aptazyme described by Breaker et al. ***(15)***. Our aptazyme reports theophylline-induced cleavage in *trans* (i.e., with an external, replaceable substrate) by fluorescence resonance energy transfer (FRET) between a donor (Cy3) and an acceptor fluorophore (Cy5) covalently linked to the substrate termini (**Fig. 1A**). Before cleavage, the donor is close to the acceptor fluorophore and FRET occurs, which is characterized by a strong emission at the acceptor wavelength of 665 nm (**Figs. 1** and **2A**). Upon substrate cleavage and product dissociation, FRET breaks down and the donor specific emission at 565 nm increases (**Figs. 1** and **2A**). This breakdown of FRET provides an amplified signal for the presence of theophylline. The chosen pair of cyanine fluorophores for FRET is compatible with our goal to apply single-molecule fluorescence microscopy ***(20,21,23)*** to the detection of analyte binding.

This chapter reviews in detail the methods and protocols to prepare our theophylline specific aptazyme and to label its substrate with fluorophores. We also include detailed protocols to characterize by FRET the binding affinity of the target, theophylline, as well as the external substrate to the aptazyme (*see* **Note 1**).

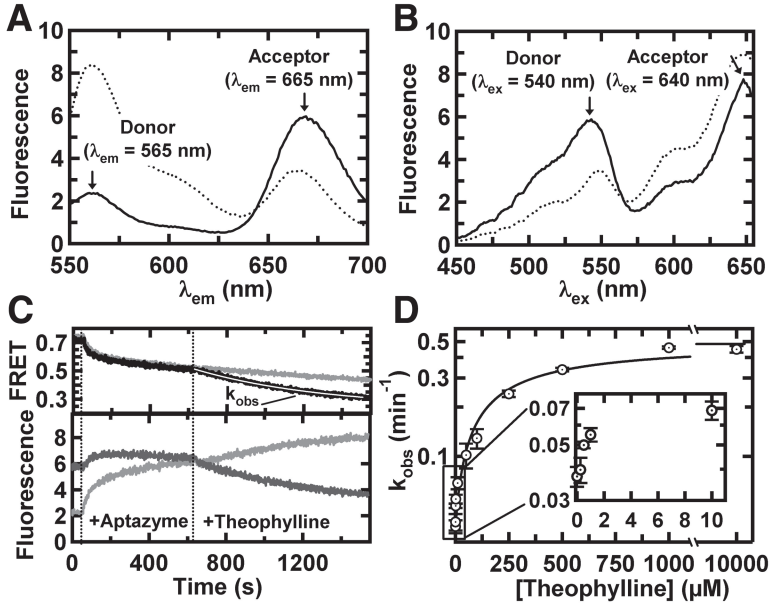

Fig. 2. Fluorescence resonance energy transfer (FRET) readout for the theophylline dependent aptazyme as basis for a biosensor. **(A)** Emission spectrum of Cy3-Cy5 doubly labeled substrate. Upon addition of the aptazyme and theophylline (dotted line), donor emission increases while acceptor emission decreases, characteristic of a FRET decrease upon substrate cleavage and product release. **(B)** Excitation spectrum of the Cy3-Cy5 doubly labeled substrate. Upon addition of the aptazyme and theophylline (dotted line), donor excitation results in a lower acceptor signal than before, characteristic of a FRET decrease upon substrate cleavage and product release. **(C)** Lower panel: Fluorescence emission time traces of the donor (dark gray measured at 565 nm) and acceptor (light gray, measured at 665 nm) fluorophores upon excitation at 540 nm. The upper panel shows the resulting FRET time trace (black). Initially the relative FRET efficiency is constant at 0.8. After 60 s the aptazyme is added and the FRET ratio decreases as a result of cleavage and product release in the absence of theophylline. After approx 600 s theophylline is added, and the FRET decrease is enhanced as a result of accelerated cleavage induced by theophylline. This decrease is fit to a single-exponential decay (white line), whose rate is k_{obs}. Addition of caffeine instead of theophylline does not cause a similar acceleration in cleavage (top panel, light gray). **(D)** Concentration dependence of the rate of FRET decrease, k_{obs}, as a function of theophylline concentration. Theophylline concentrations in the low μ*M* range are sufficient to induce a measurable rate enhancement (inset). *See* text for experimental details.

2. Materials

2.1. Aptazyme Transcription and Purification

1. Polymerase chain reaction (PCR) buffer: 10 m*M* Tris-HCl, pH 8.3, 1.5 m*M* $MgCl_2$, and 50 m*M* KCl.
2. Tris-EDTA (TE) buffer: 10 m*M* Tris-HCl, pH 7.0, 1 m*M* EDTA.
3. Tris-boric acid-EDTA (TBE) buffer: 100 m*M* Tris base, 70 m*M* boric acid, 2 m*M* EDTA.
4. Formamide gel loading buffer: 90% (v/v) formamide, 0.025% (w/v) xylene cyanol, and 0.025% (w/v) bromophenol blue in TBE buffer.
5. Buffered chloroform/isoamyl alcohol: 96% (v/v) chloroform, 4% (v/v) isoamyl alcohol. Add 1/3 vol TE buffer. Mix and allow the aqueous and organic phases to separate. Use only the chloroform/isoamyl alcohol layer (bottom).
6. Buffered phenol/chloroform: 50% (v/v) phenol, 50% (v/v) buffered chloroform/isoamyl alcohol. Add one-third volume TE buffer. Mix and allow the aqueous and organic phases to separate. Use only the phenol/chloroform/isoamyl alcohol layer (bottom).
7. Transcription buffer: 120 m*M* HEPES-KOH, pH 7.6, 30 m*M* $MgCl_2$, 40 m*M* dithiothreitol (DTT), 5 U/mL inorganic pyrophosphatase, 2 m*M* spermidine, and 0.01 % (w/v) Triton X-100.
8. Elution buffer: 0.1 m*M* EDTA, pH 8.0, 0.1% (w/v) sodium dodecyl sulfate (SDS), and 500 m*M* ammonium acetate.
9. DNA primers (Invitrogen, Carlsbad, CA).
10. *Taq* DNA polymerase (TaKaRa Biochemical, Berkeley, CA).
11. 3 *M* NaOAc, pH 5.2.
12. 100 and 80% (v/v) Ethanol.
13. Commercial T7 RNA polymerase (e.g., TaKaRa Biochemical), or purified in native form from overexpressing *Escherichia coli* strain BL31/pAR1219 ***(24)***, or purified in histidine-tagged form from overexpressing *E. coli* strain BL21/pRC9 ***(25)***.
14. DTT (e.g., Fisher Scientific).
15. Spermidine (e.g., Fisher Scientific).
16. Triton X-100 (e.g., Fisher Scientific).
17. Inorganic pyrophosphatase (Sigma-Aldrich, St. Louis, MO).
18. Vertical slab gel electrophoresis apparatus (20×16 cm^2), including glass plates, 1-mm spacers, 1-mm fitting seal, 1-mm one- or two-well comb, clamps, and aluminum plate (e.g., CBS Scientific, Del Mar, CA).
19. Centricon Plus-20 centrifugal filters (Millipore, Bedford, MA).
20. Hand-held ultraviolet (UV) lamp, wavelength 312 or 254 nm (e.g., Fisher Scientific).
21. Thin-layer chromatography (TLC) plate (20×20 cm^2) with fluorescent indicator (e.g., Fisher Scientific).
22. Empty Poly-Prep chromatography column (Bio-Rad Laboratories, Hercules, CA).

2.2. Synthetic RNA Substrate Purification and Labeling

1. High-performance liquid chromatography (HPLC) system with C_8-reversed phase column (e.g., ProStar system from Varian, Palo Alto, CA).
2. HPLC mobile phase B: 100% acetonitrile.
3. HPLC stationary phase A: 100 m*M* triethylammonium acetate, pH 7.0.
4. Synthetic RNA oligonucleotides (e.g., HHMI Biopolymer/Keck Foundation Biotechnology resource laboratory at the Yale University, School of Medicine, New Haven, CT).
5. Triethylamine trihydrofluoride (e.g., Sigma-Aldrich or Fisher Scientific).
6. N,N-dimethylformamide (e.g., Fisher Scientific; optional).
7. 1-butanol.
8. 100 and 80% (v/v) ethanol.
9. 14-mL Falcon centrifuge tube (e.g., Fisher Scientific).
10. Dimethyl sulfoxide (e.g., Fisher Scientific).
11. Cy5-succinimidyl ester (Amersham Biosciences, Piscataway, NJ).

2.3. Steady-State FRET Assays

1. Standard buffer: 50 m*M* Tris-HCl, pH 7.5, 10 m*M* $MgCl_2$, and 25 m*M* DTT as oxygen scavenger.
2. AMINCO-Bowman 2 spectrofluorometer (Thermo Electron Corporation, Rochester, NY), or similar.
3. Quartz cuvet, 3-mm pathlength, 200 µL vol (Starna Cells, Atascadero, CA).
4. Theophylline (e.g., Sigma-Aldrich).

2.4. Time-Resolved FRET Assays

1. Frequency doubled Nd:VO_4 pump laser, e.g., Millenia Xs-P (Spectra-Physics, Mountain View, CA).
2. Tunable Ti:Sapphire picosecond laser operating at 980 nm, e.g., Tsunami (Spectra-Physics, Mountain View, CA).
3. Pulse picker/frequency doubler module, e.g., model 3980-2 (Spectra-Physics).
4. Sample compartment Koala (ISS, Champaign, IL).
5. Microchannel plate photomultiplier tube, model R3809U-50 (Hamamatsu Corporation, Bridgewater, NJ).
6. Time-correlated single-photon counting card, SPC-630 (Becker and Hickl, Berlin, Germany).
7. Quartz cuvet, 10-mm sides, 80 µL volume (Starna Cells).
8. Emission band-pass filter, 25 mm diameter and 4-mm thick, HQ570/10m (Chroma, Rockingham, VT).
9. Fused silica filter-mimic, 25 mm diameter and 4 mm thick (Edmunds Industrial Optics, Barrington, NJ).
10. Circular neutral density variable filter (Edmund Industrial Optics).

2.5. Radioactive Cleavage Assays

1. Stop solution: 50 m*M* EDTA, pH 7.5, 90% (v/v) formamide, 0.025% (w/v) xylene cyanol, and 0.025% (w/v) bromophenol blue in TBE buffer.
2. Polynucleotide Kinase and Kinase buffer (Promega, Madison, WI).
3. [γ-^{32}P]-ATP, 500 µCi (ICN Biomedicals, Costa Mesa, CA).
4. Centrispin-10 column (e.g., Princeton Separations, Adelphia, NJ).
5. PhosphorImager (e.g., Storm 840 PhosphorImager with ImageQuant software [Amersham Biosciences]) with Phosphor Screens.

3. Methods

3.1. Aptazyme Transcription and Purification

The aptazyme can be conveniently transcribed in vitro from a DNA template because it does not contain any site-specific chemical modification that would require incorporation by solid phase synthesis. The following protocols describe in detail how to transcribe and purify the theophylline specific aptazyme (**Fig. 1**) starting from the initial design of the DNA template. This procedure is schematically depicted in **Fig. 3**.

3.1.1. DNA Template Design

The length of the DNA template strands necessary to transcribe the theophylline specific aptazyme exceeds the maximum length recommended for efficient DNA synthesis (approx 60 nt) (*see* **Note 2**). Therefore, the full-length DNA template is generated from two shorter DNA primers by overlap-extension PCR (**Fig. 3**). Two DNA primers for overlap extension PCR are designed in the following way. First, the 5' primer (5'-CAG **TAA TAC GAC TCA CTA TA**G GCA *ACA CTG ATG AGC CTT ATA CCA GCC GGA AAC G*-3') contains the T7 promoter sequence (bold) followed by 35 nucleotides corresponding to the aptazyme's 5'-end sequence (**Fig. 3**). (It is worth mentioning that a U in the RNA transcript corresponds to a T in the DNA template.) Second, the 3' primer (5'-CCC GTT TCG ACG TCT GCC AAG GGC *CGT TTC CGG CTG GTA TAA GGC TCA TCA GTG T*-3') contains 55 nucleotides complementary to the aptazyme's 3'-end sequence (**Fig. 3**, the overlapping sequences are shown in italics). DNA primers for the overlap extension PCR are best obtained by retro-design: Firstly, the desired sequence of the duplex DNA template is determined, and secondly, the primers of the overlap extension PCR are derived by trimming to a sufficiently short length, while keeping approx 30 overlapping nucleotides between them.

3.1.2. Overlap-Extension PCR

1. In a thin-walled PCR microcentrifuge tube, mix 2 µ*M* of each primer, 0.3 m*M* of each deoxyribonucleoside triphosphates, and 0.05 U/µL *Taq* DNA polymerase in

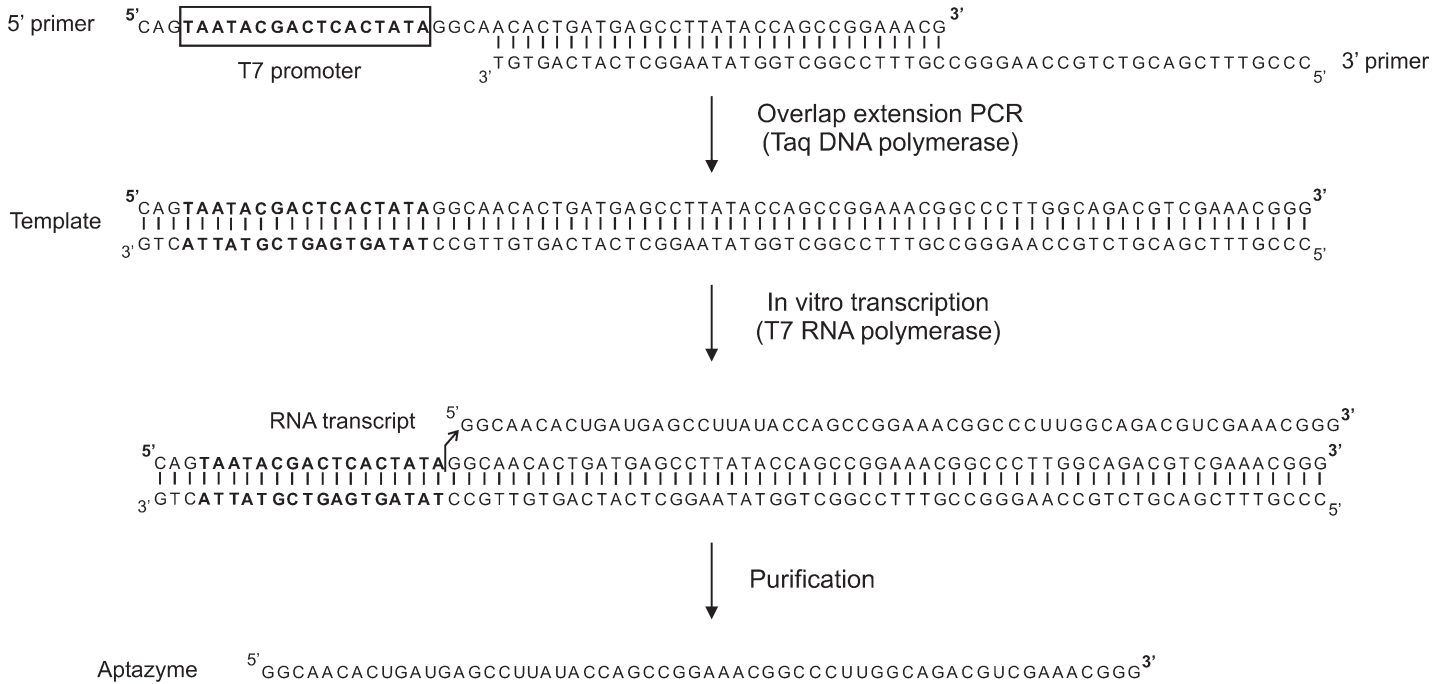

Fig. 3. Schematic depiction of aptazyme synthesis and purification. First, the DNA template is generated by overlap extension polymerase chain reaction of the 5' and 3' DNA primers. The T7 promoter region is boxed and highlighted in bold. Then, in vitro transcription of the DNA template generates a single-stranded RNA, which is gel purified. *See* text for experimental details.

PCR buffer (final volume in tube: 100 µL; the reaction can be scaled up by using multiple tubes).
2. In a thermocycler, incubate the reaction mix at 94°C for 30 s, 55°C for 30 s, 72°C for 30 s. Cycle four times.
3. Extract the PCR products with 1 vol (100 µL) of buffered phenol/chloroform. Microcentrifuge for 1 min at 12,000*g* and 4°C. Carefully remove the aqueous layer (top) with a pipet, and transfer to a fresh tube. Repeat extraction procedure once.
4. Add sodium acetate to a final concentration of 300 m*M* (i.e., 1/10 vol, or 10 µL, of 3 *M* NaOAc) and 2–2.5 vol (220–275 µL) of 100% ethanol. Precipitate the DNA for 2 h at –20°C.
5. Centrifuge for 30 min at 12,000*g* and 4°C to pellet precipitated DNA. Decant supernatant, wash pellet with 80% ethanol, decant supernatant again, and dry DNA in a Speedvac evaporator.
6. Dissolve in a suitable volume of water (50–200 µL).
7. Obtain a UV-Vis absorption spectrum from 220 to 800 nm of a 1:100 (v/v) diluted sample. Calculate DNA concentration from the peak absorption at 260 nm, after background subtraction of the absorption at 320 nm (one corrected A_{260} unit = 0.050 µg/µL double stranded PCR product).

3.1.3. In Vitro Transcription and Purification

1. In a microcentrifuge tube, mix 200 n*M* of the DNA template from the overlap extension PCR (**Subheading 3.1.2.**), inorganic pyrophosphatase to a final concentration of 5 U/mL, each rNTP to a final concentration of 7.5 m*M*, and T7 RNA polymerase to a final concentration of 6 U/µL in transcription buffer (final volume: typically 2 mL).
2. Incubate overnight (16–20 h) at 37°C.
3. Concentrate reaction to approx 200 µL by ultracentrifugation through a Centricon Plus-20 centrifugal filter.
4. Add 200 µL formamide gel loading buffer. Purify on one lane of a denaturing polyacrylamide gel (20% [w/v] acrylamide, 8 *M* urea). Electrophorese gel at 25 W constant power until the bromophenol blue band reaches the end of the gel (approx 1.5–2 h).
5. Visualize the RNA by UV shadowing: place the gel, plastic-wrapped, over a TLC plate, and irradiate with a hand-held UV-lamp (312 nm, or 254 nm if higher sensitivity is required; use protective eyewear) in the dark. The TLC plate is fluorescent when excited with UV light. In those regions of the gel where the RNA is located, it will absorb the UV light, decreasing the fluorescence and, thus, appearing as a shadow. Mark the band position using a permanent marker on the plastic wrap, then excise the product band in the light using a clean razor blade.
6. Slice each band into small pieces (approx 2×2 mm^2). Transfer the pieces into an empty Poly-Prep chromatography column, add 4 mL elution buffer, and tumble on a tube shaker overnight (16–20 h) at 4°C.
7. Transfer solution to a 15-mL Falcon tube by gravitational flow through the column frit, extract SDS with 1 vol (4 mL) of buffered chloroform/isoamyl alcohol.

Table 1
Spectroscopic Properties for Some Commonly Used Fluorophores

Fluorophore	Excitation (nm)	Emission (nm)	Quantum yield
FAM	490	520	0.71
HEX	538	551	n/a
TAMRA	554	573	0.28
Cy3	540	565	0.13
Cy5	640	665	0.18

FRET pairs are composed of a donor and an acceptor fluorophore. The emission spectrum of the donor fluorophore must overlap with the excitation spectrum of the acceptor fluorophore. Typical fluorophore pairs are FAM as donor with TAMRA, HEX, or Cy3 as acceptor, or Cy3 as donor with Cy5 as acceptor ***(26)***.

Centrifuge for 5 min at 10,000*g* and 4°C, remove carefully the aqueous layer (top) with a pipet, and transfer to a fresh Falcon tube.

8. Add sodium acetate to a final concentration of 300 m*M* (i.e., 1/10 vol, or 400 µL of 3 *M* NaOAc) and 2–2.5 vol (8.8–11 mL) of 100% ethanol. Precipitate RNA for 2 h at –20° C.
9. Centrifuge for 10 min at 10,000*g* and 4°C to pellet precipitated RNA. Decant supernatant, wash pellet with 80% ethanol, decant supernatant again, and dry RNA in a Speedvac evaporator.
10. Dissolve RNA in suitable volume of water (50–200 µL).
11. Obtain a UV-Vis absorption spectrum of a 1:100 (v/v) diluted sample from 220 to 800 nm. Calculate RNA concentration from the peak absorption at 260 nm, background-subtracted with the absorption at 320 nm (one A_{260} unit = 0.037 µg/µL single-stranded RNA). Store at –20°C.

3.2. Synthetic RNA Substrate Purification and Labeling

To perform FRET experiments, the substrate must be labeled with a donor (Cy3) and an acceptor fluorophore (Cy5) (**Fig. 1**). The former is incorporated during synthesis at the 5'-end, whereas the latter must be attached post-synthetically to a modified primary amine at the 3'-end using a Cy5-succinimidyl ester ***(16)*** (*see* **Note 3**). Similarly, we can also label a noncleavable substrate analog, whose 2'-hydroxyl group at the cleavage site has been replaced by a 2'-methoxy group to prevent cleavage, and 5' and 3' products strands (**Fig. 1A**) for binding and dissociation studies. This protocol describes the deprotection and purification of the synthesized RNA substrate, followed by the 3'-amine labeling reaction (*see* **Note 4**).

3.2.1. Choice of Fluorophores

A variety of fluorophores can be used as FRET pairs. Some of these fluorophores are listed in **Table 1**. It is important to choose an appropriate

fluorophore pair for the experiment to be performed. A typical pair for bulk solution experiments is fluorescein and tetramethylrhodamine as donor and acceptor, respectively. This pair is widely used, stable and offers a very good quantum yield of fluorescence (**Table 1**). For this work, however, we chose Cy3 and Cy5 as donor and acceptor, respectively. This pair offers a wide spectral separation of the donor and acceptor signals, and it is the best fluorophore pair for measurements on immobilized single molecules ***(20)***, which are ultimately the smallest biosensor components imaginable.

3.2.2. Deprotection of the Tert-Butyldimethylsilyl Group

1. After the commercial vendor has already removed the base protection groups, dissolve the dried tert-butyldimethylsilyl protected 5'-Cy3-labeled RNA in 800 µL triethylamine trihydrofluoride in its original tube to avoid losses caused by tube transfer. The solubility of long RNA (>30 nt) can be increased by adding 200 µL dimethylformamide. Tumble on a tube shaker at room temperature overnight (16–20 h).
2. Add 160 µL water to quench the desilylation reaction. Transfer to a fresh Falcon tube.
3. Add 4 mL of 1-butanol, and precipitate RNA at –20°C for 45 min.
4. Centrifuge for 10 min at 10,000*g* and 4°C to pellet RNA. Gently decant the supernatant. Wash pellet with 1 mL 80% ethanol, decant supernatant, and repeat wash. Dry RNA in a Speedvac evaporator.

3.2.3. RNA Purification

Synthetic RNA is best purified by two consecutive techniques: gel electrophoresis and C_8-reversed phase HPLC. The former eliminates shorter byproducts of the synthesis, whereas the latter eliminates any byproduct from the desilylation reaction (**Subheading 3.2.1.**).

1. Dissolve the dried RNA in 200 µL formamide gel loading buffer.
2. Purify by denaturing polyacrylamide gel electrophoresis (20% [w/v] acrylamide, 8 *M* urea). Electrophorese gel at 25 W constant power until the bromophenol blue band reaches the end of the gel (approx 1.5–2 h). Keep the electrophoresis assembly in the dark (e.g., cover it using a cardboard box or wrap it with aluminum foil) to protect the donor fluorophore from ambient light.
3. Visualize the RNA by UV shadowing, excise the product bands, elute in 4 mL elution buffer, extract SDS, precipitate, and dry RNA as described in **Subheading 3.1.3., steps 5–10**, except that ATP or GTP can be added as a co-precipitant to a final concentration of 1 m*M* in the ethanol precipitation (**step 9**). The NTP is subsequently removed by HPLC purification.
4. Dissolve RNA in 100 µL water.
5. Purify by C_8-reversed phase HPLC. Begin and equilibrate the HPLC column with 100% stationary phase A. Ramp the mobile phase B from 0 to 20% in 20 min, then to 40% in 40 min, and finally to 60% in 10 min (total 70 min). Collect

appropriate fractions (*see* **Note 5**), combine them, and dry in a Speedvac evaporator. Dissolve dry RNA in appropriate volume of water (50–200 µL).
6. Calculate RNA concentration as described in **Subheading 3.1.3.**, **step 12**. Store labeled RNA at –20°C in the dark.

3.2.4. 3'-Amine Labeling Reaction and Purification

Up to 100 µg RNA can be labeled in one reaction with this protocol. It is often wise not to label more than half of the material available (**Subheading 3.2.2.**). Keep the remaining half for a second labeling reaction in case of accidental loss and to use as a singly labeled control in the time-resolved FRET assays (*see* **Note 6**).

1. Bring RNA sample to a convenient volume of 100 µL with water.
2. Extract with 1 vol (100 µL) of buffered chloroform/isoamyl alcohol as described in **Subheading 3.1.3.**, **step 8**. Transfer the aqueous (top) layer to a fresh tube.
3. Precipitate, and dry RNA as described in **Subheading 3.1.3.**, **steps 9** and **10**.
4. Dissolve RNA in 11 µL water, 75 µL 0.1 *M* $Na_2B_2O_7$, pH 8.5, and 200 µg of Cy5-succinimidyl ester pre-dissolved in 14 µL dimethyl sulfoxide.
5. Tumble on a shaker overnight (16–20 h) at room temperature.
6. Precipitate, and dry RNA as described in **Subheading 3.1.3.**, **steps 9** and **10**.
7. Purify by C_8-reversed phase HPLC, as described in **Subheading 3.2.3.**, **step 7**. If the RNA has been successfully labeled with Cy5, a second, well resolved peak appears at longer elution times, as Cy5 makes the RNA more hydrophobic. Collect appropriate fractions (*see* **Note 5**), combine them, and dry in a Speedvac evaporator. Dissolve dry RNA in appropriate volume of water (50–200 µL).
8. Calculate RNA concentration as described in **Subheading 3.1.3.**, **step 12**. Store labeled RNA in aliquots at –20°C in the dark.

3.3. Steady-State FRET Assays

Steady-state fluorescence assays are performed to monitor the breakdown of FRET upon substrate cleavage as well as to measure rates of binding and dissociation of the substrate and the cleavage products. The following protocols describe in detail how to perform such assays and quantify the results.

3.3.1. Cleavage Assays

1. Prepare 150 µL substrate solution with 50 n*M* Cy3-Cy5 doubly labeled substrate in standard buffer (*see* **Note 7**).
2. Prepare 7 µL aptazyme solution with 6 µ*M* aptazyme in standard buffer. Heat at 90°C for 45 s and cool to room temperature for more than 5 min to fold RNA.
3. Prepare 7 µL theophylline solution with 3 m*M* theophylline in standard buffer.
4. Incubate solutions at 25°C for 5–15 min.
5. Load 140 µL substrate solution in a clean quartz cuvet, and place it in the sample chamber of the spectrofluorometer, thermostated at 25°C.

6. Average five emission spectra between 550 and 700 nm (8 nm slit-width) at 10 nm/s acquisition rate, while exciting at 540 nm (4 nm slit-width, **Fig. 2A**). Adjust photomultiplier tube voltage to prevent signal saturation.
7. Average five excitation spectra between 450 and 655 nm (4 nm slit width), at 10 nm/s acquisition rate, while monitoring the emission at 665 nm (8 nm slit-width, **Fig. 2B**). Adjust photomultiplier tube voltage to prevent signal saturation.
8. Measure a time trace exciting Cy3 at 540 nm (4 nm slit-width), and monitoring simultaneously the emission of Cy3 (565 nm, 8 nm slit-width) and Cy5 (665 nm, 8 nm slit-width) by continuously shifting the emission monochromator between both wavelengths (**Fig. 2C**, bottom panel). This can be done using the "intracellular probes" function on the AMINCO-Bowman 2 spectrofluorometer. A relative FRET efficiency (**Fig. 2C**, top panel) is calculated as $FRET = F_A/(F_A + F_D)$, where F_D and F_A are the donor and acceptor fluorescence emissions, respectively.
9. During the initial 60 s, the relative FRET efficiency should be constant. Then, add 5 µL aptazyme solution to the quartz cuvet and mix manually with the pipet (final aptazyme concentration: 200 n*M)* (*see* **Note 8**). Aptazyme-substrate binding is characterized by a significant decrease in the relative FRET efficiency (**Fig. 2C**, top panel) as the substrate changes from a random coil conformation to the bound structure (**Fig. 1**). Some residual cleavage of the substrate in the absence of theophylline also causes the FRET ratio to slowly decrease after binding, with a rate constant k_0. Monitor these processes in real-time for 10 min, allowing equilibrium to be reached.
10. Add 5 µL the theophylline solution to the quartz cuvet and mix manually with the pipet (final theophylline concentration: 100 µ*M)*. Monitor the theophylline induced change in relative FRET signal for 15 min. The resulting exponential decrease (**Fig. 2C**) is characteristic of the FRET breakdown upon substrate cleavage and product dissociation (**Fig. 1**).
11. Fit the measured exponential decrease to the equation $y = y_0 + Ae^{-k_{obs}t}$, where A is the amplitude and k_{obs} is the pseudo-first order rate constant.
12. Repeat the experiment for final theophylline concentrations ranging from 250 n*M* to 10 m*M*. Plot $_{obs}$ as a function of theophylline concentration, and fit to the equation $k_{obs} = k_0 + k_{max}\,[theo]/([theo] - K_{theo})$ to derive an apparent theophylline dissociation constant, K_{theo}, and a maximum observed rate, k_{max} (**Fig. 2D**). The observed rate constant in the absence of theophylline, k_0, can be held constant to the experimentally determined value (*see* **Note 9**). The binding isotherm obtained by this method provides a calibration curve to calculate the concentration of theophylline in an unknown solution.

A good biosensor for theophylline must be able to discriminate between the target molecule, theophylline, and the ubiquitous caffeine. Caffeine and theophylline only differ structurally by a single additional methyl group on the N7 of the purine ring (**Fig. 1B**). An important control experiment is performed using this same protocol but replacing theophylline with 1 m*M* caffeine. Addition of caffeine does not lead to the characteristic FRET decrease induced by theophylline (**Fig. 2C**).

3.3.2. Substrate and Product Binding and Dissociation Rates

Desired properties of RNA-based biosensor components include fast substrate binding, slow substrate dissociation, and fast product dissociation; this ensures that ligand-induced substrate cleavage is the rate-limiting step. The binding rates of the substrate and the product can be measured using steady-state FRET, as described in **Subheading 3.3.1.**, and a noncleavable substrate or product analog. Here we describe detailed protocols for such measurements.

3.3.2.1. Substrate Binding Rate Constant

1. Prepare 150 µL substrate analog solution with 5 n*M* Cy3-Cy5 doubly labeled noncleavable substrate analog in standard buffer (*see* **Note 7**).
2. Prepare 7 µL aptazyme solution with 1.5 µ*M* aptazyme in standard buffer. Heat at 90°C for 45 s and cool to room temperature for more than 5 min to fold RNA.
3. Incubate solutions at 25°C for 5–15 min.
4. Load 145 µL substrate solution in a clean quartz cuvet, and place it in the sample chamber of the spectrofluorometer, thermostated at 25°C.
5. Measure averaged emission and excitation spectra as described in **Subheading 3.3.1.**, **steps 6** and **7**.
6. Measure a time trace as described in **Subheading 3.3.1.**, **step 8**.
7. During the initial 60 s, the relative FRET efficiency should be constant. Then, add 5 µL aptazyme solution to the quartz cuvet and mix manually with a pipet (final aptazyme concentration: 50 n*M*, *see* **Note 8**). Binding of substrate to the aptazyme is characterized by an exponential decrease in the relative FRET efficiency.
8. Fit the measured exponential decrease to the equation $y = y_0 + Ae^{-k_{obs}t}$, where A is the amplitude and k_{obs} is the pseudo-first order rate constant.
9. Repeat the experiment for final aptazyme concentrations varying between 50 and 100 n*M*. Plot k_{obs} as a function of aptazyme concentration, and an apparent bimolecular binding rate constant, $k_{on} = (1.09 \pm 0.02)\ 10^7\ min^{-1}M^{-1}$, is derived as the slope ***(15)***.

3.3.2.2. Substrate Dissociation Rate Constant

Substrate dissociation rate constants are measured by first forming an aptazyme-noncleavable substrate analog complex, then "chasing" the noncleavable substrate using a large excess of unlabeled DNA analog (of the same sequence as the RNA substrate, but unlabeled) that sequesters free aptazyme liberated upon dissociation of the aptazyme-noncleavable substrate analog complex. Our aptazyme-noncleavable substrate analog complex dissociates too slowly to be measured by a chase experiment at room temperature. Therefore, the substrate dissociation rate constant was measured at higher temperatures, and then extrapolated to 25°C using an Arrhenius plot.

1. Prepare 7 µL DNA solution with 1.5 m*M* DNA substrate analog in standard buffer (*see* **Note 7**).

2. Assemble the ribozyme-noncleavable substrate analog complex as described in **Subheading 3.3.2.1.**, **steps 1–7**, but modify **step 3** to incubate solutions at 35°C for approx 15 min. Allow equilibrium to be reached.
3. Add 5 µL DNA analog solution to the quartz cuvet and mix manually with a pipet (final DNA concentration: 50 µ*M*, *see* **Note 8**). Substrate dissociation is characterized by an exponential increase in the relative FRET efficiency.
4. Fit the measured exponential increase to the equation $y = y_0 + Ae^{-k_{off}t}$, where A is the amplitude and k_{off} is the dissociation rate constant.
5. Repeat the experiment at temperatures varying between 30 and 40°C. Make an Arrhenius plot by drawing $\ln(k_{off})$ as a function of 1/T (K^{-1}). The extrapolation of the dissociation rate constant to 25°C yields an upper estimate for k_{off} 0.21 min^{-1} ***(15)***.

The ratio k_{off}/k_{on} yields an upper estimate for the equilibrium dissociation constant K_D 18.8 n *M*, indicating that bound substrate has a lower probability to dissociate than to be cleaved, as expected for an efficient biosensor component.

3.3.2.3. Product Dissociation Rate Constant

Fast 5' product dissociation rate constants are measured with a chase experiment at room temperature. First the aptazyme-5' product complex is formed with excess aptazyme and then the product is chased with a high concentration of DNA product analog (of the same sequence as the RNA 5' product, but unlabeled).

1. Prepare 150 µL product solution with 5 n*M* Cy3-labeled 5' product in standard buffer (*see* **Note 7**).
2. Prepare 7 µL aptazyme solution with 24 µ*M* aptazyme in standard buffer. Heat at 90°C for 45 s and cool to room temperature approx 5 min to fold RNA.
3. Prepare 7 µL DNA solution with 1.5 m*M* DNA product analog in standard buffer.
4. Incubate solutions at 25°C for 1–5 min.
5. Load 140 µL product solution in a clean quartz cuvet, and place it in the sample chamber of the spectrofluorometer, thermostated at 25°C. Then, add 5 µL aptazyme solution to the quartz cuvet and mix manually with the pipet (final aptazyme concentration: 800 n*M*, *see* **Note 8**). Allow to equilibrate.
6. Measure a time trace exciting Cy3 at 540 nm (4 nm slit-width), and monitoring Cy3 emission at 565 nm (8 nm slit-width).
7. During the initial 60 s, the Cy3 emission should be constant. Then, add 5 µL DNA solution to the quartz cuvet and mix manually with the pipet (final product analog concentration: 50 µ*M*). Product dissociation is characterized by an exponential decrease (quenching) in Cy3 emission.
8. Fit the measured exponential decrease to the equation $y = y_0 + Ae^{-k_{off}t}$, where A is the amplitude and k_{off} = 4.2 min^{-1} is the 5' product dissociation rate constant ***(15)***.

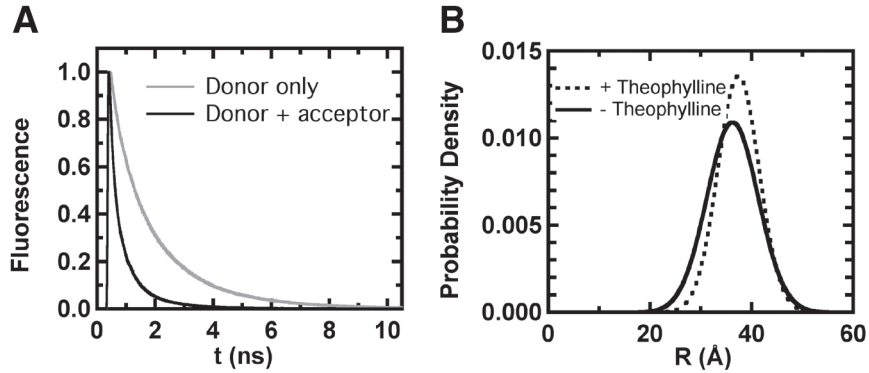

Fig. 4. Time-resolved fluorescence resonance energy transfer (FRET) reveals slight changes in global conformation of the aptazyme-non-cleavable substrate analog complex upon theophylline addition. **(A)** Normalized fluorescence decay of the donor fluorophore (Cy3) in the absence (gray) and in the presence (black) of the acceptor fluorophore (Cy5). In the presence of the acceptor, the donor excitation decays more rapidly owing to FRET. **(B)** Resulting donor-acceptor distance distribution, P(R), in the absence (dashed line; mean distance = 37 ± 1 Å, full width at half maximum = 9 ± 2 Å) and in the presence (solid line; mean distance = 36 ± 1 Å, full width at half maximum = 12 ± 2 Å) of theophylline. The global structure of the theophylline aptamer changes only slightly in the presence of theophylline. *See* text for experimental details.

The dissociation rate constant of the 3' product could not be measured because it is too fast. Such fast dissociation of both products is ideal to ensure that theophylline-induced substrate cleavage is rate-limiting for the overall reaction pathway (**Fig. 1A**).

3.4. Time-Resolved FRET Assay

To test the structural impact of theophylline the global structure of the theophylline aptazyme in the presence and in the absence of theophylline can be determined by measuring the distance between the donor and acceptor fluorophores. For this purpose, the donor fluorescence lifetime is measured in the presence and in the absence of the acceptor fluorophore. The resulting lifetime differences are used to derive a Gaussian distance distribution between the two fluorophores (**Fig. 4**).

1. Prepare an 80 µL solution with 1 µ*M* Cy3-Cy5 doubly labeled noncleavable substrate analog and 3 µ*M* aptazyme in standard buffer (*see* **Note 7**). This complex does not undergo catalysis so that only conformational changes induced by theophylline are monitored.

2. Prepare an 80 µL solution with 1 µ*M* Cy3 singly labeled noncleavable substrate analog and 3 µ*M* aptazyme in standard buffer.
3. Heat both solutions at 90°C for 45 s, and cool to room temperature approx 5 min to fold RNA.
4. Prepare 12 µL solution with 17 m*M* theophylline in standard buffer.
5. Incubate all solutions for approx 15 min at 25°C.
6. Operate the Nd:VO_4 pump laser at 9 W to pump the Ti:Sapphire laser.
7. Set the Ti:Sapphire output wavelength to 980 nm. Adjust the Gires-Tournois Interferometer (GTI) to optimize mode-locking. Pulse width should be approx 2 ps, and the corresponding spectral width is approx 0.8 nm.
8. Set the model 3980-2 pulse picker/frequency doubler to pick down the output of the Ti:Sapphire laser to 4 MHz, and generate its second harmonic for a final excitation wavelength of 490 nm.
9. Place a quartz cuvet containing 80 µL of dilute nondairy creamer in the ISS sample compartment of the lifetime fluorometer, thermostated at 25°C, and decrease the excitation intensity with a filter wheel so that the detection frequency does not exceed 40 KHz (1% of the 4 MHz pulse train from the Ti:Sapphire laser) to avoid counting artifacts. Use the fused silica filter mimic and place the emission polarizer at magic angle. Measure an instrument function up to approx 40,000 counts peak intensity.
10. Place a quartz cuvet with 80 µL singly labeled aptazyme-noncleavable substrate analog complex in the lifetime fluorometer. Replace the filter mimic by the emission filter, and adjust excitation intensity for a detection frequency of ≤40 KHz. Measure the fluorescence decay up to approx 40,000 counts peak intensity (**Fig. 4A**).
11. Place a quartz cuvet with 80 µL doubly labeled aptazyme-noncleavable substrate analog complex in the lifetime fluorometer. Adjust excitation intensity for a detection frequency of ≤40 KHz, and measure the fluorescence decay up to approx 40,000 counts peak intensity (**Fig. 4A**).
12. Add 5 µL theophylline solution to the cuvets containing the singly and doubly labeled complexes. Incubate approx 15 min, and repeat measurements.
13. Use the instrument function to deconvolute all fluorescence decays.
14. Fit the deconvoluted donor-only decay functions to the sum of three exponential decays $I_D = \sum_{i=1,2,3} \alpha_i \mathrm{epx}\ \{-(t/\tau_i)\}$.
15. Fit the deconvoluted doubly labeled decay functions to the equation $I_{DA}(t) = \int_{(\mathrm{integral})}(R)\sum_{i=1,2,3}\alpha_i \exp[-\{t/\tau_i\}\{1 + (R_0/R)^6\}]dR$, where α_i and τ_i are the donor-only decay parameters, *R0* is the the Förster distance at which the FRET efficiency is 50%, and *P(R)* is the distance distribution. The latter is modeled as a three-dimensional weighted Gaussian, $P(R) = 4\pi R^2 N \exp\{-\sigma(R-\mu)^2\}$, where N is a normalization constant, and σ and μ describe the shape of the Gaussian (**Fig. 4B**).
16. Repeat the fitting procedure for the fluorescence decays in the presence of theophylline (**Fig. 4B**).

3.5. Radioactive Cleavage Assay

Alternatively to fluorescent detection, theophylline-induced cleavage activity of the aptazyme can be detected using a radioactively labeled substrate. This assay provides an important control for the possible effect of the fluorophore labels on aptazyme function. This protocol describes the [γ-^{32}P]-ATP-labeling reaction of the unmodified substrate and the radioactive cleavage assay.

3.5.1. Radioactive Substrate Labeling

1. In a microcentrifuge tube, prepare a 25 µL reaction with 400 n*M* unmodified substrate, 2.5 µL fresh [γ-^{32}P]-ATP, and 0.5 µL polynucleotide kinase in kinase buffer.
2. Incubate 30 min at 37°C.
3. Add 25 µL water to reaction tube.
4. Load the 50 µL into a primed Centrispin-10 column. Spin at 600*g* for 2 min to separate the labeled substrate from excess [γ-^{32}P]-ATP by gel filtration.
5. Collect the filtrate and add 350 µL water. Store this 5'-[^{32}P] labeled substrate at –20°C for up to 2 wk from the date of certification of the [γ-^{32}P]-ATP.

3.5.2. Single-Turnover Cleavage Assay

1. In a first microcentrifuge tube, prepare 75 µL of a solution with 12 µL of the 5'-[^{32}P] labeled substrate (*see* **Subheading 3.5.1.**) in standard buffer.
2. In a second microcentrifuge tube, prepare 75 µL with 400 n*M* aptazyme, and 2 m*M* theophylline in standard buffer.
3. Heat both tubes at 70°C for 2 min, and slowly cool to room temperature approx 5 min.
4. Incubate in a 25°C water bath for 2 min. Mix 2.5 µL of the first and second tubes with 10 µL stop solution for a zero time point. Mix 70 µL of the first tube with 70 µL of the second to initiate the reaction. Start taking the time.
5. Remove 5 µL from the reaction tube and mix with 10 µL stop solution at appropriate time points.
6. Separate the uncleaved substrate from the products by denaturing polyacrylamide gel electrophoresis (20% acrylamide, 8 *M* urea). Electrophorese gel at 25 W constant power, until the bromophenol blue band has migrated for two-thirds of the gel length (approx 1–1.5 h).
7. Expose Saran-wrapped gel to a Phosphor Screen, and quantify the fraction cleaved using a PhosphorImager.
8. Fit the fraction cleaved as described in **Subheading 3.3.1.**, **step 11** to obtain an observed cleavage rate constant, k_{obs}.
9. Repeat the experiment for final theophylline concentrations varying between 250 n*M* and 10 m*M*, and fit the observed pseudo-first order time-courses as described in **Subheading 3.3.1.**, **step 12** to obtain a theophylline binding constant, K_{theo}.

In the case of our theophylline aptazyme, the observed cleavage rates, k_{obs}, and the theophylline binding constant, K_{theo}, obtained by this protocol were very similar to those obtained with fluorescence detection (**Fig. 2C**) ***(15)***. This proved that the fluorophore labels do neither affect the catalytic activity of this aptazyme nor its ability to detect theophylline.

4. Notes

1. For all procedures water is always deionized and autoclaved. When working with RNA always wear gloves to prevent degradation by "finger" RNases.
2. The overlap extension PCR step can be eliminated when the DNA template is sufficiently short to be synthesized directly.
3. It is possible to inverse the fluorophore-labeling scheme proposed in this chapter. However, labeling a Cy5 containing RNA with Cy3 results in less well resolved HPLC peaks because Cy3 changes the RNA hydrophobicity less than Cy5. If such a labeling strategy is required, it is possible to improve the HPLC peak resolution by using a shallower mobile phase gradient than the one described under **Subheading 3.2.3.**, **step 7**.
4. Keep RNA always wrapped with aluminum foil throughout the procedure to protect the 5'-Cy3 fluorophore from ambient light.
5. We strongly recommended running an analytical HPLC prior to loading the preparative HPLC. A 1:20 diluted sample (final volume: 100 µL) is usually sufficient for the analytical HPLC. This allows the RNA elution times to be known ahead of time so that an appropriate window of fractions around the desired peak can be collected.
6. The Cy5-succinimidyl ester labeling reaction is inhibited in the presence of residual triethylammonium acetate from the previous HPLC purification step. Therefore, it is essential to first eliminate any residual triethylammonium acetate by chloroform extraction.
7. In order to suppress fluorophore photobleaching caused by singlet oxygen dissolved in solution, we typically add 25 m*M* DTT as an oxygen scavenger. For maximum effectiveness, DTT must be added freshly every time a new solution is prepared, therefore, we do not recommend adding it to buffers that are stored for extended periods of time.
8. Use long gel loading tips for optimum mixing.
9. In this work, the observed cleavage rate constant in the absence of theophylline (k_0) is included to derive the binding isotherm. Consequently, a slightly different theophylline-binding constant, K_{theo}, is reported compared to our previous work ***(15)***.

Acknowledgments

We would like to thank all current and former members of the Walter laboratory for stimulating discussions and helpful suggestions while developing these experiments, particularly Philip T. Sekella for pioneering these studies.

This work was supported by grants from the NIH (GM62357) and the American Chemical Society (PRF no. 37728-G7) to NGW.

References

1. Hendeles, L. and Weinberger, M. (1983) Theophylline. A "state of the art" review. *Pharmacotherapy* **3,** 2–44.
2. Wilson, D. S. and Szostak, J. W. (1999) In vitro selection of functional nucleic acids. *Annu. Rev. Biochem.* **68,** 611–647.
3. Hoffman, D., Hesselberth, J., and Ellington, A. D. (2001) Switching nucleic acids for antibodies. *Nat. Biotechnol.* **19,** 313–314.
4. Breaker, R. R. (2002) Engineered allosteric ribozymes as biosensor components. *Curr. Opin. Biotechnol.* **13,** 31–39.
5. Silverman, S. K. (2003) Rube Goldberg goes (ribo)nuclear? Molecular switches and sensors made from RNA. *RNA* **9,** 377–383.
6. Winkler, W. C., Nahvi, A., Roth, A., Collins, J. A., and Breaker, R. R. (2004) Control of gene expression by a natural metabolite-responsive ribozyme. *Nature* **428,** 281–286.
7. Soukup, G. A. and Breaker, R. R. (1999) Design of allosteric hammerhead ribozymes activated by ligand-induced structure stabilization. *Structure. Fold. Des.* **7,** 783–791.
8. Soukup, G. A. and Breaker, R. R. (1999) Engineering precision RNA molecular switches. *Proc. Natl. Acad. Sci. USA* **96,** 3584–3589.
9. Soukup, G. A. and Breaker, R. R. (1999) Nucleic acid molecular switches. *Trends Biotechnol.* **17,** 469–476.
10. Soukup, G. A. and Breaker, R. R. (2000) Allosteric nucleic acid catalysts. *Curr. Opin. Struct. Biol.* **10,** 318–325.
11. Soukup, G. A., DeRose, E. C., Koizumi, M., and Breaker, R. R. (2001) Generating new ligand-binding RNAs by affinity maturation and disintegration of allosteric ribozymes. *RNA* **7,** 524–536.
12. Soukup, G. A., Emilsson, G. A., and Breaker, R. R. (2000) Altering molecular recognition of RNA aptamers by allosteric selection. *J. Mol. Biol.* **298,** 623–632.
13. Zimmermann, G. R., Wick, C. L., Shields, T. P., Jenison, R. D., and Pardi, A. (2000) Molecular interactions and metal binding in the theophylline-binding core of an RNA aptamer. *RNA* **6,** 659–667.
14. Wedekind, J. E. and McKay, D. B. (1998) Crystallographic structures of the hammerhead ribozyme: relationship to ribozyme folding and catalysis. *Annu. Rev. Biophys. Biomol. Struct.* **27,** 475–502.
15. Sekella, P. T., Rueda, D., and Walter, N. G. (2002) A biosensor for theophylline based on fluorescence detection of ligand-induced hammerhead ribozyme cleavage. *RNA* **8,** 1242–1252.
16. Walter, N. G. (2001) Structural dynamics of catalytic RNA highlighted by fluorescence resonance energy transfer. *Methods* **25,** 19–30.
17. Walter, N. G., Harris, D. A., Pereira, M. J., and Rueda, D. (2001) In the fluorescent spotlight: global and local conformational changes of small catalytic RNAs. *Biopolymers* **61,** 224–242.

18. Pereira, M. J., Harris, D. A., Rueda, D., and Walter, N. G. (2002) Reaction pathway of the trans-acting hepatitis delta virus ribozyme: a conformational change accompanies catalysis. *Biochem.* **41,** 730–740.
19. Harris, D. A., Rueda, D., and Walter, N. G. (2002) Local conformational changes in the catalytic core of the trans-acting hepatitis delta virus ribozyme accompany catalysis. *Biochem.* **41,** 12,051–12,061.
20. Zhuang, X., Kim, H., Pereira, M. J., Babcock, H. P., Walter, N. G., and Chu, S. (2002) Correlating structural dynamics and function in single ribozyme molecules. *Science* **296,** 1473–1476.
21. Bokinsky, G., Rueda, D., Misra, V. K., et al. (2003) Single-molecule transition-state analysis of RNA folding. *Proc. Natl. Acad. Sci. USA* **100,** 9302–9307.
22. Rueda, D., Wick, K., McDowell, S. E., and Walter, N. G. (2003) Diffusely bound Mg^{2+} ions slightly reorient stems I and II of the hammerhead ribozyme to increase the probability of formation of the catalytic core. *Biochem.* **42,** 9924–9936.
23. Rueda, D., Bokinsky, G., Rhodes, M. M., Rust, M. J., Zhuang, X., and Walter, N. G. (2004) Single-molecule enzymology of RNA: essential functional groups impact catalysis from a distance. *Proc. Natl. Acad. Sci. USA* **101,** 10,066–10,071.
24. Grodberg, J. and Dunn, J. J. (1988) ompT encodes the Escherichia coli outer membrane protease that cleaves T7 RNA polymerase during purification. *J. Bacteriol.* **170,** 1245–1253.
25. He, B., Rong, M., Lyakhov, D., et al. (1997) Rapid mutagenesis and purification of phage RNA polymerases. *Protein Expr. Purif.* **9,** 142–151.
26. Walter, N. G. and Burke, J. M. (2000) Fluorescence assays to study structure, dynamics, and function of RNA and RNA-ligand complexes. *Methods Enzymol.* **317,** 409–440.